

Coupled Simulations of the 20th-Century including External Forcing

Caspar M. Ammann^{*†}, Jeffrey T. Kiehl^{*}, Charles S. Zender[‡],
Bette L. Otto-Bliesner^{*}, Raymond S. Bradley[†]

^{*}Climate and Global Dynamics Division, National Center for Atmospheric
Research¹, Boulder, CO, USA

[†]Department of Geosciences, University of Massachusetts, Amherst, MA, USA

[‡]Department of Earth System Science, University of California, Irvine, CA, USA

Submitted to :

Journal of Climate

as *Letter*

October 26, 2002

Corresponding author address:

Dr. Caspar Ammann

National Center for Atmospheric Research, Climate and Global Dynamics Division,
1850 Table Mesa Drive, Boulder, CO 80305, USA

Tel: (303) 497-1705 , Fax: (303) 497-1348

e-mail: ammann@ucar.edu

¹The National Center for Atmospheric Research is sponsored by the National Science Foundation.

ABSTRACT

New coupled experiments with the National Center for Atmospheric Research (NCAR) Climate System Model (CSM) covering the period from 1870 to 2000 are presented. They incorporate a detailed treatment of volcanic aerosols together with solar irradiance as well as anthropogenic changes in atmospheric composition and tropospheric aerosol loading. The temporal evolution of the natural forcing is compared with anthropogenic factors and globally averaged perturbations of climate are compared with observations. Only a few large eruptions perturb the system significantly beyond the background noise, but these events contribute substantially to the interannual to decadal variability. The addition of volcanic aerosol significantly improved the simulation of surface temperature changes of the 20th-Century. Analysis of the computed external forcing in these simulations support a significant natural contribution to the warming in the first half of the 20th-Century. Since 1963, the substantial forcing from the large volcanic eruptions of Agung (1963), El Chichón (1982) and Pinatubo (1991) basically offset solar irradiance changes and natural forcing is not playing an important role in the recent warming.

1 Introduction

The climatic evolution of the 20th-Century contains two substantial warming episodes on the global scale, one from around 1910 to 1945 and the other after \sim 1975 (Folland and co authors, 2001, a). Simulations with General Circulation Models (GCMs) that incorporate the changes in atmospheric greenhouse gas concentrations (GHG) and tropospheric aerosol loading (e.g. Stott et al., 2000; Delworth and Knutson, 2000; Dai et al., 2001) consistently show better agreement with trends in observations (and among each other) in the latter part of the century. This is due to the radiative forcing from greenhouse gases, which increase in a significant way only after about 1960. Prior to this increase, the largely unforced models (GHG and tropospheric aerosol are rather low) and observations are not expected to exhibit a high interannual correlation since most of the variance arises from internal (stochastic) climate variability from a host of processes (see e.g. Mann and Park, 1994). Thus, observed decadal variations are almost impossible to reproduce in a coupled climate model which exhibits its own internal variability. Nevertheless, it is possible that single ensemble members can show very similar behavior (Delworth and Knutson, 2000).

Long-term solar variations have previously been proposed to contribute significantly to the warming early in the century, and also, at least to some degree, in recent decades (Lean et al., 1995; Tett et al., 1999; Andronova and Schlesinger, 2000). At the frequency of the 11-year sunspot cycle, the solar forcing is more difficult to associate with climatic variations, but new studies found correlations in observational data (e.g., van Loon and Shea, 1999) and might offer indications for a mechanism of how the signal could be transmitted from the stratosphere downward into the troposphere (Balachandran et al., 1999; Shindell et al., 2001).

Explosive volcanism is another significant natural forcing factor. Aerosol clouds

composed mostly of sulfuric acid can strongly impact Earth’s radiative balance (Kelly and Sear, 1984; Bradley, 1988; McCormick et al., 1995). Particularly large tropical events that spread the aerosol over both hemispheres are able to influence the global climate. Only a small number of events produce large enough clouds (Dutton and Bodhaine, 2001) and because their lifetime is generally short, a climate effect is limited to a few years. But an extension of cooling from individual events has been proposed through close temporal spacing of big events (Lamb, 1970; Robock, 1978; Porter, 1986). Such series of events in the past include for example periods in the 17th and the early 19th-Century. These sequences of large events coincided with some of the cool episodes of *The Little Ice Age* (Bradley, 2000). The last 150 years also contained two periods with relatively high volcanic activity (1883 to 1912 and 1963 to 1991) separated by a very quiescent period.

The influence of external forcing is not restricted to perturbations of the radiative balance alone. Additionally, dynamical responses to the spatial distribution of the forcing (both horizontally and vertically) could cause interactions with internal modes of climate (Palmer, 1999). Such a case of modification of the internal climate variability has been proposed for the anthropogenic greenhouse forcing on the North Atlantic Oscillation (NAO, Shindell et al., 1999) and similar effects could arise from the natural external forcings (Kirchner et al., 1999; Shindell et al., 2001). In particular, the episodically appearing volcanic forcing could influence this major mode resulting in a typical regional pattern in addition to the purely radiative effects from the aerosol (Robock, 2000). This modification could potentially extend the signal beyond the period where significant amounts of aerosol are present.

In the following Section (2), we give an overview of the experiments performed with a coupled GCM and describe the applied natural and anthropogenic forcing data. Section 3.1 discusses the forcing imposed on the climate by the different natural

and anthropogenic components. In 3.2, we focus on the climatic impact from the volcanic aerosol and then evaluate natural versus anthropogenic forcing in a historical experiment (Section 3.3). Emphasis is given to the multi-decadal contributions to the climate. Section 3.4 presents the models performance in capturing an aspect of high-latitude circulation that has recently gained more attention. Finally, Section 4 summarizes the importance of external forcing during the 20th-Century and a short discussion on remaining uncertainties is given.

2 Model and Forcing Data

We used the latest *Paleo-Version* (Otto-Bliesner and Brady, 2001) of the coupled *National Center for Atmospheric Research (NCAR) Climate System Model (CSM)*. Compared to CSM-1 (Boville and Gent, 1998, and references therein), this configuration contains updated versions of the standard components. The atmosphere (Kiehl et al., 1996, 1998) was run with a spectral resolution of T31 (or 3.75 x 3.75 degrees in a transform grid) with 18 levels in the vertical, ranging from the surface to ~35 km. The radiative fluxes are computed hourly using a δ -Eddington approach in 19 short-wave bands (SW) from 0.2 to 5 μm and longwave fluxes (LW) between 5 and 50 μm are derived in 6 broadbands. The land model distinguishes between specified vegetation types and contains a comprehensive treatment of surface processes (Bonan, 1998). The ocean model (Gent et al., 1998) was run using a grid containing 25 vertical levels with a spacing of 3.6° in longitude and the latitudinal resolution changes from 0.9 degrees in the tropics (10°N - 10°S) to 1.8 degrees in latitudes > 30° N and S. It was updated as described in Boville et al. (2001). Together with a background vertical diffusivity of 0.15 cm^2s^{-1} , these changes improved a number of deficiencies compared to previous versions (see Boville et al., 2001) and generates reasonable El Niño events

(Otto-Bliesner and Brady, 2001; Meehl et al., 2001). The sea ice model includes ice thermodynamics based on the three-layer model of Semtner and ice dynamics based on the cavitating fluid rheology of Flato and Hibler (Weatherly et al., 1998). All components exchange fluxes through a flux coupler (Bryan et al., 1997). The model does not require flux corrections (Boville et al., 2001).

Three experiments are presented.

CON: Unforced control experiment with atmospheric composition held fixed at 1870 conditions (Houghton et al., 1996). Even after a spin-up integration of over 100 years (70 of which in coupled mode), the control experiment exhibited a slight surface imbalance of roughly 0.5 Wm^{-2} and the small trend of 0.0156 K per decade was removed. The other experiments show anomalies relative to the control.

VOL: Same as CON but with an added volcanic aerosol history. The volcanic forcing data was derived mostly from visible optical depth data of Stothers (1996) and Sato et al. (1993) but included a simple parameterization of the seasonally changing meridional aerosol transport. Because the evolution of aerosol clouds from each event was estimated using the relatively well known parameters of month-of-the-eruption and the maximum-sulfate-mass (assumed to have developed four months after the eruption), the resulting dataset does not suffer from significantly changing detail in available observations of these clouds. Although data with much higher precision would be available over the satellite period since 1979 (El Chichon and Pinatubo), the selected method offers a first order approach to a consistent description of the aerosol through time. Here, only events with clearly measured perturbations to the radiative budget since the 1880s are included. This is in line with the findings of Bluth et al. (1997), Stothers (1996) and Dutton and Bodhaine (2001) who showed that only few events perturb the global radiative balance noticeably. A fixed mid-sized Pinatubo aerosol size distribution of sulfuric acid ($75\% \text{ H}_2\text{SO}_4 + 25\% \text{ H}_2\text{O}$)

with $r_{eff} = 0.45 \mu\text{m}$ and $\sigma = 1.25$ (after Stenchikov et al., 1998) was used in the detailed treatment of stratospheric particles.

HIST: The historical experiment was forced with a full set of external and anthropogenic forcing. For greenhouse gases, the model directly distinguishes between CO_2 , CH_4 , N_2O , CFC-11 and CFC-12 (additional halocarbons are included through appropriate scaling of CFC-11 and CFC-12). Their temporal evolution were the same as in previous experiments with CSM as discussed in (Dai et al., 2001). A fixed ozone distribution (with seasonal cycle) from Wang et al. (1995) was applied in all experiments. A prescribed 3-dimensional evolution of natural (assumed constant) and anthropogenic sulfate aerosol was taken from an interactive sulfate simulation (Rasch et al., 2000), which was based on a seasonally varying SO_2 emission cycle in the mid-1980s and scaled over time by the emission history. Only the direct forcing is incorporated (Kiehl et al., 2000). The Hoyt and Schatten (1993) forcing series was used to describe the change in solar constant (consistent with previous experiments at NCAR), scaled to a present day solar irradiance of 1367 Wm^{-2} . The volcanic forcing was the same as in VOL.

The individual forcing time series are summarized in Figure 1. Compared to the concentrations of greenhouse gases, the uncertainties in the spatial and temporal evolution of tropospheric aerosol (amount and composition!) is quite large (e.g., Satheesh and Ramanathan, 2000). Equally, the long-term evolution of solar irradiance before the satellite period (1979-present) contains a significant amount of uncertainty, although variations within the 11-year sunspot cycle are somewhat better constrained (Beer et al., 2000). The volcanic forcing, on the other hand, can be approximated for decadal averages to within roughly 20% (Hansen et al., 1997), but for individual eruptions uncertainties of up to a factor of 2 might apply.

3 Results

3.1 Radiative Forcing

The upper plot in Figure 2 presents the evolution of the annual TOA total net flux (SW and LW) in VOL. Since the volcanoes were the only cause for changes in the radiative budget beyond internal variations, this time series represents the volcanic forcing as it is translated from the specified mid-visible aerosol optical depth shown in Figure 1 into a radiative perturbation in the climate simulation. It includes all feedbacks represented in the model (positive and negative ones). The short-dashed lines embracing the host of the TOA net fluxes are the two-standard-deviations (2σ) of this field from the undisturbed control run CON. A few deviations both above and below these levels can be seen as expected. Large negative deviations exist during periods of large volcanic perturbations of the radiative fluxes. The eruptions are marked as triangles on top and the bottom of the Figure. The largest events perturb the annual TOA net fluxes beyond 1 Wm^{-2} and reach the -2σ level. The long-dashed line represents the -2σ levels of VOL. Only the largest eruptions perturb the radiative budget below this level. A number of years also exhibit a positive deviation beyond 2σ of the control, but none reach $+1 \text{ Wm}^{-2}$, the 2σ level of VOL. The largest positive values are quite often reached after the recovery from volcanic perturbations suggesting that the climate system could be overshooting somewhat in its attempt to restore radiative balance. On the decadal scale, the volcanic perturbation to the radiative balance varies between -0.6 and $+0.1$ or $+0.2 \text{ Wm}^{-2}$, which is in good agreement with Hansen and Sato (2001).

The dominant component in the solar forcing on climate lies in its low frequency variation. Figure 1 shows the estimated changes in the solar constant by Hoyt and

Schatten (1993). Other reconstructions (Lean et al., 1995; Solanki and Fligge, 1999) show similar, though somewhat smaller changes over time. The slow increasing trend over the 130 years is of the order of 3 or 4 Wm^{-2} for individual years, and about 2 Wm^{-2} for some decadal averages. This is about twice as large as average variations on the 11-year sunspot cycle. In the following calculations of total natural forcing, we conservatively estimated the solar component by dividing the annual irradiance by 4 as compensation for the solar zenith angle and scaled it with the co-albedo ($1 - \alpha_p$, with $\alpha_p = 0.3$).

The anthropogenic forcing components change more slowly in time. Dai et al. (2001) showed that tropospheric sulfate forcing compensates the effects from increasing greenhouse gases up to about 1970 (calculated offline, Kiehl et al., 2000). Subsequently, the tropospheric aerosol loading as shown in Figure 1 starts to level off (due to reduction in sulfur content in oil and gasoline) but greenhouse gases increase rapidly. By the end of the 20th-Century, the combined anthropogenic forcing reaches about 1.25 Wm^{-2} ($+1.8 \text{ Wm}^{-2}$ from GHG and -0.55 Wm^{-2}). Note, we only included the direct aerosol effect.

3.2 Volcanic impact on climate

The climate response to the volcanic forcing is shown in the lower plot of Figure 2. The dashed line represents the 2σ level following a cubic spline. The five largest volcanic eruptions (Krakatau 1883, Santa Maria 1902, Agung 1963, El Chichón 1982 and Pinatubo 1991) can readily be recognized in the surface temperature series through a marked cooling. This cooling is generally surpassing the 2σ level. The smaller events can generally also be recognized as coolings, but only if their timing is known. They are basically indistinguishable from the internal climate variability on the interannual

time scale.

Interestingly, the climatic perturbations of high-latitude events (shown in Figure 2 as open triangles) such as the large 1912 eruption of Katmai-Novarupta, Alaska, are much less important on the global scale than could be implied by their aerosol mass. The forcing is too restricted to the high latitudes and the removal process is faster than for tropical events. Therefore, it can be concluded that only a handful of large tropical eruptions, with aerosol injections into both hemispheres leave a clear imprint on the evolution of climate, while high-latitude events generate a more regional response.

In terms of low frequency variations, VOL exhibits two significant cooling episodes, one initiated by Krakatau with additional minor contributions from the event in 1890 and Santa Maria in 1902, and the other during the last 40 years of the simulation. This can be seen in the 10-year running average as well as in the evolution of the cubic spline shown in Figure 2. It has been suggested that periods with enhanced volcanic activity could influence background trends in climate (Lamb, 1970; Robock, 1978; Porter, 1986). The results from VOL support the existence of such an influence. While the period 1883 to 1905 is dominated by the very large Krakatau event and a contribution to the low frequency climate evolution from the other events is masked, the sequence of eruptions after 1963 is perturbing the system enough so that the climate simulated in CSM cannot fully recover, and a cooling trend of almost 0.2 K results.

3.3 20th-Century simulation

The upper plot in Figure 3 shows the simulation of the 20th-Century (red line) using volcanic and solar variations as natural as well as the set of greenhouse gases and tropospheric sulfate as anthropogenic forcing. The surface temperature is compared

to different observational time series (Jones et al., 2001; Hansen et al., 1999; Quayle et al., 1999), which are shown in their annual range. These time series are anomalies to their 1961-90 average. They overlay the $\pm 2\sigma$ range from CON shown in the gray shaded horizontal bar. Without forcing, the simulation would be expected to remain within this region. The simulation and observations show very similar deviations from this: At the end of the 19th- and early 20th-Century, the simulated surface temperature drops below the range after years of three large volcanic eruptions. The general agreement with the observations is quite good with the exception of the 1880s, where the simulated effect of Krakatau is much larger than the observed cooling. Subsequently, the temperatures increase, reaching a maximum in the 1940s. Note, the large observed cooling in 1918 was due to a large La Niña event, which was not simulated in CSM. The period between 1950 and 1975 is slightly cooler than the 1940s. In the final 25 years, the rapid temperature increase is only interrupted by two large volcanic coolings from El Chichón and Pinatubo. The cooling from El Chichón is somewhat larger in the simulation than observed, probably due to the absence of the strong El Niño (see the positive spike in the observations, and also discussion in Wigley, 2000). The eruption of Pinatubo also occurred during an El Niño event, though the magnitude was much weaker and cannot explain the difference to the simulation. One reason could be the specified peak optical depth in the tropics of 0.35 which is more than 15% larger than in Sato et al. (1993). Note, in the model, an average El Niño event can only account for slightly less than 0.1°K global average temperature.

On the interannual time scale, the major volcanic eruptions described in VOL are generally well simulated and can still be recognized. The 1890 eruption (Stothers, 1996) is simulated somewhat clearer in HIST than VOL, but Agung (1963) now exhibits a smaller response. The different responses in the individual runs to the

same forcing are highlighting the influence of internal variability. The other 4 large events are similar in magnitude. Knowing the timing of the small events indicates synchronous cooling in HIST and the observations, though a clear identification of a volcanic signal against internal variability is very difficult.

The bottom plot of Figure 3 shows 25-year averaged segments of forcing separated in combined natural (volcanic and solar) and anthropogenic components (GHG and tropospheric sulfate). There is good agreement between forcing and climate evolution plotted above. After the (overly) strong cooling due to Krakatau, the climatic trend in HIST contains a warming of 0.2 to 0.3 K from about 1910 to 1940. Another strong increase in surface temperature of +0.5 K, interrupted only by accentuated fluctuations by large eruptions, occurs after 1970. In-between, the simulated temperature changes very little or even cools slightly. This overall trend closely resembles the combined anthropogenic and natural forcing shown in the bars at the bottom in Figure 3. While the combined anthropogenic forcing of greenhouse gases and tropospheric aerosol essentially cancel until 1970, increased solar irradiance from 1910 to 1945 and a virtual absence of strong volcanic perturbations allow for this warming. The subsequent decrease in solar irradiance and the reappearance of volcanic events after 1963 are in line with the simulated trends in temperature. Although solar irradiance is high again in the last decades of the century, large volcanic eruptions are efficiently counteracting this positive forcing. This effect can also be inferred from the climate response. The prolonged cooling (i.e. beyond the individual years of perturbation) in the last decades of VOL (see Figure 2 suggests that the warming trend of HIST is brought in line with observations due to the decadal cooling component from closely spaced eruptions. Thus, the rapid increase of the greenhouse gas forcing after about 1970 must be causing the coupled climate to warm substantially in the final 30 years of the simulation. Only in the few years with significant volcanic

forcing is the warming interrupted. This large variation within the natural component of the climate forcing can be illustrated for the last 25-year segment between 1975 and 2000. Inclusion of volcanic aerosol reduces the natural forcing from roughly 0.3 Wm^{-2} (solar) to below 0.1 Wm^{-2} . Neglecting the volcanoes, the globally averaged solar forcing would amount to roughly one half of the combined anthropogenic forcing during these 25 years. Nevertheless, by the year 2000, this factor drops to below one quarter ($+1.25 \text{ Wm}^{-2}$ anthropogenic vs. $+0.3 \text{ Wm}^{-2}$ solar only, see also Lean et al., 1995).

3.4 North Atlantic Circulation and Volcanoes

The experiments highlight the need for inclusion of the natural forcing in simulations of the instrumental time period. That the benefit is not restricted to the improved simulation of the long-term trends, is apparent when considering at the decadal evolution of temperature. The fluctuations common to both observations and HIST are quite remarkable. Prolonged cooling after an eruption is suggestive of a volcanic pacemaker role, even for eruptions that do not show up significantly above the noise level of the radiative balance (see Figure 3). That this contribution to the internal climate variations is non-trivial can be seen in the high correlation coefficient between HIST and the observations ($r^2 = 0.725$ with Jones et al. (2001) and 0.77 with Hansen et al. (1999)). While the direct radiative effects diminish rather quickly, a possible 'resetting' of internal modes of climate variability could result in an extension of the parallel evolution before internal noise causes divergence between the time series.

One candidate mechanism is the NAO. Defant (1924) suggested an influence of volcanic dust on the circulation patterns in the North Atlantic region. Lamb (1970) later extended the studies and found an initial decrease in the Westerlies during the

months immediately following tropical eruptions (due to decreased temperature gradients between the low and high-latitudes) and a subsequent increase in the strength of the Westerlies. Kodera (1995) and most recently Perlwitz and Graf (2001) have studied the mechanisms of high-latitude circulation variations also in the vertical dimension, and modeling experiments (Graf et al., 1993; Kirchner et al., 1999; Shindell et al., 2001) have reproduced its response to volcanic perturbations through changes in vertical wave propagation and increased strength of the polar vortex. This increased circulation in winter time manifests itself at the surface through a warming over a large part of the Northern Hemisphere continents (Groisman, 1992; Robock and Mao, 1992, 1995; Kelly et al., 1996). Thus, the volcanic impact is not only radiative in nature but contains an important dynamical component (Graf et al., 1993; Kirchner et al., 1999; Robock, 2002). CSM does exhibit similar trends in high-latitude circulation and produces the winter warming reasonably well.

One measure of the circulation that is directly tied to such a response is the NAO index. Table 1 compares the evolution of the NAO computed after Hurrell (1995) for the superposed set of the seven largest tropical eruptions since 1870 in the three simulations with observations (Hurrell, 1995). Years -1 and 0 represent the NAO during two winter prior to the eruptions, 1 is the first winter after the events. A common behavior can be recognized between VOL, HIST and Hurrell. In the first winter after the eruptions, the NAO increases due to the volcanic aerosol. Other than in the observations, this increase is continued for one more year in VOL and HIST. Subsequently, both observations and the simulations show a decrease in the NAO. An even closer correlation to the observations was achieved in a four-member ensemble simulation of the large Krakatau eruption. The clear influence of the volcanic aerosol on the NAO is well reproduced.

4 Discussion and conclusions

The first coupled NCAR-CSM experiment of the 20th-Century using a full set of external forcings reproduces the main features of the observed temperature evolution since 1870. Compared to previous simulations (Meehl et al., 2000; Dai et al., 2001), the addition of a detailed treatment of volcanic aerosol brings the simulation into better agreement with the observations (at least in global quantities) both on interannual to decadal time scales.

Figure 4 shows that the magnitude of the simulated temperature decrease from tropical events is well correlated with the mass of sulfuric acid injected into the lower tropical stratosphere. A linear relationship between changes in the visible optical depth and surface temperature has been proposed by Pollack et al. (1976). Rampino and Self (1984) and Sigurdsson (1990) isolated the sulfate mass as the most reliable index in relation with the temperature. Our simulations show that this generally used simplification seems to work well with the exception of Krakatau (1883), undoubtedly the largest eruption of the last 150 years. Independent estimates of Krakatau stratospheric aerosol mass range from 30 to 75 Mt (see e.g. summary by Stothers, 1996). Here, a maximum of 52 Mt of sulfuric acid was applied (January 1884, computed from the aerosol optical depth and the known particle size dependent mass extinction coefficient) in order to match the mid-latitude evolution described in Stothers (1996). While the climate signal is small in the observations, the model simulations consistently produce a cooling between 0.55 and 0.85 K (range from a four member ensemble, not shown). Given the demonstrated importance of the large eruptions, resolution of the discrepancy between the observational and simulated cooling may involve including evolving particle sizes depending on the sulfate mass (see e.g. Pinto et al., 1989). These issues with a particular focus on the simulation of Krakatau will

be discussed in more detail elsewhere.

Another important issue concerning the volcanic forcing is whether or not a series of volcanic eruptions can impose a low frequency impact on climate. While the strong cooling resulting from Krakatau requires further investigation, the last four decades of the 20th-Century demonstrate a clear long-term impact of closely spaced volcanic eruptions (see Figure 3). Similarly, the absence of events in the mid-part of the 20th century results in a mid century warming. How much of that warming could be due to 'volcanic recovery' (Lamb, 1970; Kondratyev and Galindo, 1997; Stott et al., 2000) is speculative. The comparison of VOL with the range in CON suggests a contribution of roughly 0.1 K. From the radiative balance, some over-compensation can be found, but it does not exceed a few years (at the most). More ensemble experiments are needed to verify this effect.

Overall, the simulation of 20th-Century climate using a complete set of natural and anthropogenic forcings (HIST) captures the main aspects of global climate trends very well. The inclusion of natural forcing factors strongly increases the quality of the simulations. The long-term trend is improved through better representation of the warming early in the 20th-Century. The cancelling effects of volcanic eruptions and solar irradiance after 1970 allow a direct association of most of the simulated and observed warming to the influence of atmospheric greenhouse gas concentrations during the last decades of the 20th-Century. Although the quality in our knowledge of both forcing and observations decreases back in time, particularly before 1900 (Jones et al., 1986; Madden et al., 1993; Folland et al., 2001), the successful reproduction of the climatic evolution using independently derived estimates of the external forcing factors lends confidence to the coupled climate models ability to simulate the instrumental time period. The only exception is the large difference between observations and simulated response to the eruption of Krakatau in 1883. Further investigations

are underway to understand this particular event. An extension to the way in which stratospheric aerosols are prescribed in CSM might be required. Other improvements could include the spectral resolution of changes in the solar irradiance and evolving ozone concentrations rather than a fixed distribution. But a higher vertical resolution in the stratosphere might be needed for these effects to play a significant role (Shindell et al., 1999). Also various indirect effects of tropospheric aerosol and presence of additional (particularly absorbing) species should be considered.

References

- Andronova, N. and M. Schlesinger, 2000: Causes of global temperature changes during the 19th and 20th century. *Geophysical Research Letters*, **27**, 2137–2140.
- Balachandran, N. K., D. Rind, P. Lonergan, and D. T. Shindell, 1999: Effects of solar cycle variability on the lower stratosphere and the troposphere. *Journal of Geophysical Research*, **104**, 27321–27339.
- Beer, J., W. Mende, and R. Stellmacher, 2000: The role of the sun in climate forcing. *Quaternary Science Reviews*, **19**, 403–415.
- Bluth, G. J. S., W. I. Rose, I. E. Sprod, and A. J. Krueger, 1997: Stratospheric loading of sulfur from explosive volcanic eruptions. *The Journal of Geology*, **105**, 671–683.
- Bonan, G., 1998: The land surface climatology of the NCAR land surface model coupled to the NCAR Community Climate Model. *Journal of Climate*, **11**, 1307–1326.
- Boville, B. and P. Gent, 1998: The NCAR Climate System Model, version one. *Journal of Climate*, **11**, 1115–1130.
- Boville, B., J. Kiehl, P. Rasch, and F. Bryan, 2001: Improvements to the NCAR CSM-1 for transient climate simulations. *Journal of Climate*, **14**, 164–179.
- Bradley, R., 2000: 1000 years of climate change. *Science*, **288**, 1353–1355.
- Bradley, R. S., 1988: The explosive volcanic eruption signal in Northern Hemisphere continental temperature records. *Climatic Change*, **12**, 221–243.

- Bryan, F., B. Kauffman, W. Large, and P. Gent: 1997, The NCAR CSM Flux Coupler. Technical Report NCAR/TN-424+STR, NCAR.
- Dai, A., T. Wigley, B. Boville, J. Kiehl, and L. Buja, 2001: Climates of the Twentieth and Twenty-First Centuries simulated by the NCAR Climate System Model. *Journal of Climate*, **14**, 485–519.
- Defant, A., 1924: Die Schwankungen der atmosphärischen Zirkulation über dem nordatlantischen Ozean im 25-jährigen Zeitraum 1881-1905. *Geografiska Annaler*, **6**, 13–41.
- Delworth, T. and T. Knutson, 2000: Simulation of early 20th century global warming. *Science*, **287**, 2246–2250.
- Dutton, E. G. and B. Bodhaine, 2001: Solar irradiance anomalies caused by clear-sky transmission variations above Mauna Loa: 1958-99. *Journal of Climate*, **14**, 3255–3262.
- Folland, C. and co authors: 2001, *Observed Climate Variability and Change*, chapter 2.
- Folland, C., N. Rayner, S. Brown, T. Smith, S. Shen, D. Parker, I. Macadam, P. Jones, N. Nicholls, and D. Sexton, 2001: Global temperature change and its uncertainties since 1861. *Geophysical Research Letters*, **28**, 2621–2624.
- Gent, P., F. Bryan, G. Danabasoglu, S. Doney, W. Holland, W. Large, and J. McWilliams, 1998: The NCAR Climate System Model global ocean component. *Journal of Climate*, **11**, 1287–1306.
- Graf, H.-F., I. Kirchner, A. Robock, and I. Schult, 1993: Pinatubo eruption winter climate effects: model versus observations. *Climate Dynamics*, **9**, 81–93.

- Groisman, P. Y., 1992: Possible regional climate consequences of the Pinatubo eruption: An empirical approach. *Geophysical Research Letters*, **19**, 1603–1606.
- Hansen, J. and M. Sato, 2001: Trends of measured climate forcing agents. *Proceedings of the National Academy of Science*, **98**, 14778–14783.
- Hansen, J. E., R. Ruedy, J. Glascoe, and M. Sato, 1999: GISS analysis of surface temperature change. *Journal of Geophysical Research*, **104**, 30997–31022.
- Hansen, J. E., M. Sato, and R. Ruedy, 1997: Radiative forcing and climate response. *Journal of Geophysical Research*, **102**, 6831–6864.
- Houghton, J., L. Meira Filho, B. Callander, N. Harris, A. Kattenberg, and K. Maskell, eds.: 1996, *Climate Change 1995. The science of climate change*. Contribution of WG I to the Second Assessment Report of the Intergovernmental Panel on Climate Change, Cambridge University Press, Cambridge, UK.
- Hoyt, D. V. and K. H. Schatten, 1993: A discussion of plausible solar irradiance variations, 1700-1992. *Journal of Geophysical Research*, **98**, 18,895–18,906.
- Hurrell, J. W., 1995: Decadal trends in the North Atlantic Oscillation: Regional temperatures and precipitation. *Science*, **269**, 676–679.
- Jones, P., T. Osborn, K. Briffa, C. Folland, E. Horton, L. Alexander, D. Parker, and N. Rayner, 2001: Adjusting for sampling density in grid box land and ocean surface temperature time series. *Journal of Geophysical Research*, **106**, 3371–3380.
- Jones, P., S. Raper, R. Bradley, H. Diaz, P. Kelly, and T. Wigley, 1986: Northern Hemisphere surface air temperature variations: 1851-1984. *Journal of Climate and Applied Meteorology*, **25**, 161–179.

- Kelly, P. M., P. D. Jones, and P. Jia, 1996: The spatial response of the climate system to explosive volcanic eruptions. *Journal of Climatology*, **16**, 537–550.
- Kelly, P. M. and C. B. Sear, 1984: Climatic impact of explosive volcanic eruptions. *Nature*, **311**, 740–743.
- Kiehl, J., J. Hack, G. Bonan, B. Boville, B. Briegleb, D. Williamson, and P. Rasch: 1996, Description of the NCAR Community Climate Model (CCM3). Technical Report NCAR/TN-420+STR, National Center for Atmospheric Research, Boulder, Colorado.
- Kiehl, J., J. Hack, G. Bonan, B. Boville, D. Williamson, and P. Rasch, 1998: The National Center for Atmospheric Research Community Climate Model: CCM3. *Journal of Climate*, **11**, 1131–1149.
- Kiehl, J. T., T. Schneider, P. Rasch, M. Barth, and J. Wong, 2000: Radiative forcing due to sulfate aerosols from simulations with the National Center for Atmospheric Research Community Climate Model, Version 3. *Journal of Geophysical Research*, **105**, 1441–1457.
- Kirchner, I., G. L. Stenchikov, H.-F. Graf, A. Robock, and J. C. Antuna, 1999: Climate model simulation of winter warming and summer cooling following the 1991 Mount Pinatubo volcanic eruption. *Journal of Geophysical Research*, **104**, 19039–19055.
- Kodera, K., 1995: On the origin and nature of interannual variability of the winter stratospheric circulation in the Northern Hemisphere. *Journal of Geophysical Research*, **100**, 14077–14087.

- Kondratyev, K. and I. Galindo: 1997, *Volcanic Activity and Climate*. Studies in Geophysical Optics and Remote Sensing, A. Deepak Publishing, 382pp. pp.
- Lamb, H. H., 1970: Volcanic dust in the atmosphere; with a chronology and assessment of its meteorological significance. *Transactions of the Royal Philosophical Society of London*, **A266**, 425–533.
- Lean, J., J. Beer, and R. S. Bradley, 1995: Reconstruction of solar irradiance since 1610: Implications for climate change. *Geophysical Research Letters*, **22**, 3195–3198.
- Madden, R., D. Shea, G. Branstator, J. Tribbia, and R. Weber, 1993: The effects of imperfect spatial and temporal sampling on estimates of the global mean temperature: Experiments with model data. *Journal of Climate*, **6**, 1057–1066.
- Mann, M. E. and J. Park, 1994: Global-scale modes of surface temperature variability on interannual to century timescales. *Journal of Geophysical Research*, **99**, 25819–25833.
- McCormick, M. P., L. Thomason, and C. R. Trepte, 1995: Atmospheric effects of the Mount Pinatubo eruption. *Nature*, **373**, 399–404.
- Meehl, G., W. Collins, B. Boville, J. Kiehl, T. Wigley, and J. Arblaster, 2000: Response of the NCAR Climate System Model to increased CO₂ and the role of physical processes. *Journal of Climate*, **13**, 1879–1898.
- Meehl, G., P. Gent, J. Arblaster, B. Otto-Bliener, E. Brady, and A. Craig, 2001: Factors that affect the amplitude of El Niño in global coupled climate models. *Climate Dynamics*, **17**, 515–526.

- Otto-Bliesner, B. and E. Brady, 2001: Tropical Pacific variability in the NCAR Climate System Model. *Journal of Climate*, **14**, 3587–3607.
- Palmer, T., 1999: A nonlinear dynamical perspective on climate prediction. *Journal of Climate*, **12**, 575–591.
- Perlwitz, J. and H.-F. Graf, 2001: Troposphere-stratosphere dynamic coupling under strong and weak polar vortex conditions. *Geophysical Research Letters*, **28**, 271–274.
- Pinto, J. P., R. P. Turco, and O. B. Toon, 1989: Self-limiting physical and chemical effects in volcanic eruption clouds. *Journal of Geophysical Research*, **94**, 11165–11174.
- Pollack, J. B., O. B. Toon, C. Sagan, A. Summer, B. Baldwin, and W. van Camp, 1976: Volcanic explosions and climatic change: a theoretical assessment. *Journal of Geophysical Research*, **81**, 1071–1083.
- Porter, S. C., 1986: Pattern and forcing of Northern Hemisphere glacier variations during the last Millennium. *Quaternary Research*, **26**, 27–48.
- Quayle, R. G., T. C. Peterson, A. N. Basist, and C. S. Godfrey, 1999: An operational near-real-time global temperature index. *Geophysical Research Letters*, **26**, 333–335.
- Rampino, M. R. and S. Self, 1984: Sulphur-rich volcanic eruptions and stratospheric aerosols. *Nature*, **310**, 677–679.
- Rasch, P. J., M. C. Barth, J. T. Kiehl, S. E. Schwartz, and C. M. Benkovitz, 2000: A description of the global sulfur cycle and its controlling processes in the National

- Center for Atmospheric Research Community Climate Model, Version 3. *Journal of Geophysical Research*, **105**, 1367–1385.
- Robock, A., 1978: Internally and externally caused climate change. *Journal of the Atmospheric Sciences*, **35**, 1111–1122.
- 2000: Volcanic eruptions and climate. *Reviews of Geophysics*, **38**, 191–219.
- 2002: The climatic aftermath. *Science*, **295**, 1242–1244.
- Robock, A. and J. Mao, 1992: Winter warming from large volcanic eruptions. *Geophysical Research Letters*, **12**, 2405–2408.
- 1995: The volcanic signal in surface temperature observations. *Journal of Climate*, **8**, 1086–1103.
- Satheesh, S. K. and V. Ramanathan, 2000: Large differences in tropical aerosol forcing at the top of the atmosphere and Earth’s surface. *Nature*, **405**, 60–63.
- Sato, M., J. E. Hansen, M. P. McCormick, and J. B. Pollack, 1993: Stratospheric aerosol optical depth, 1850-1990. *Journal of Geophysical Research*, **98**, 22987–22994.
- Shindell, D., R. Miller, G. Schmidt, and L. Pandolfo, 1999: Simulation of recent northern winter climate trends by greenhouse-gas forcing. *Nature*, **399**, 452–455.
- Shindell, D., G. Schmidt, R. Miller, and D. Rind, 2001: Northern Hemisphere winter climate response to greenhouse gas, ozone, solar, and volcanic forcing. *Journal of Geophysical Research*, **106**, 7193–7210.
- Sigurdsson, H., 1990: Evidence of volcanic loading of the atmosphere and climate response. *Palaeogeography, Palaeoclimatology, Palaeoecology*, **89**, 277–289.

- Solanki, S. K. and M. Fligge, 1999: A reconstruction of total solar irradiance since 1700. *Geophysical Research Letters*, **26**, 2465–2468.
- Stenchikov, G. L., I. Kirchner, A. Robock, H.-F. Graf, J. C. Antua, R. G. Grainger, A. Lambert, and L. W. Thomason, 1998: Radiative forcing from the 1991 Mount Pinatubo volcanic eruption. *Journal of Geophysical Research*, **103**, 13837–13857.
- Stothers, R. B., 1996: Major optical depth perturbations to the stratosphere from volcanic eruptions: Pyrheliometric period, 1881-1960. *Journal of Geophysical Research*, **101**, 3901–3920.
- Stott, P., S. Tett, G. Jones, M. Allen, J. Mitchell, and G. Jenkins, 2000: External control of 20th-century temperature by natural and anthropogenic forcing. *Science*, **290**, 2133–2137.
- Tett, S. F. B., P. Stott, M. Allen, W. Ingram, and J. Mitchell, 1999: Causes of twentieth-century temperature change near the Earth's surface. *Nature*, **399**, 569–572.
- van Loon, H. and D. J. Shea, 1999: A probable signal of the 11-year solar cycle in the troposphere of the Northern Hemisphere. *Geophysical Research Letters*, **26**, 2893–2896.
- Wang, W.-C., X.-Z. Liang, D. M.P., D. Pollard, and S. Thompson, 1995: Atmospheric ozone as a climate gas. *Atmospheric Research*, **37**, 247–256.
- Weatherly, J., B. Briegleb, W. Large, and J. Maslanik, 1998: Sea ice and polar climate in the NCAR CSM. *Journal of Climate*, **11**, 1472–1486.
- Wigley, T., 2000: ENSO, volcanoes and record-breaking temperatures. *Geophysical Research Letters*, **27**, 4101–4104.

Figure Captions

Figure 1 Specified boundary conditions, from top to bottom: Annual average aerosol optical depth at $0.5 \mu\text{m}$ for the stratosphere (red); Hoyt and Schatten (1993) solar irradiance change at top of the atmosphere (blue); CO_2 concentration (green); anthropogenic emission rate of sulfur used for scaling a seasonal distribution from Rasch et al. (2000). Not shown are changes in other greenhouse gases (see text).

Figure 2 Top: The volcanic forcing is shown as the actual change in TOA radiative balance in VOL in response to aerosol and climatic perturbations. Bottom: Global annual surface temperature evolution with fitted cubic spline and added -2σ intervals from CON (short dashed, no volcanoes included) and VOL (including the volcanoes).

Figure 3 Top: Annual average anomalies (reference 1961-1990) compared to the 2σ range of CON (gray box) and to observational datasets of Jones et al. (2001), Hansen et al. (1999) and Quayle et al. (1999) shown in blue. Bottom: 25-year averaged combined natural (volcanic and solar) and anthropogenic forcing. See text for details.

Figure 4 Mass of maximum sulfuric acid in the model versus maximum temperature reduction. Note: The temperature change is an estimate with at least $\pm 0.1^\circ$ uncertainty due to internal variability.

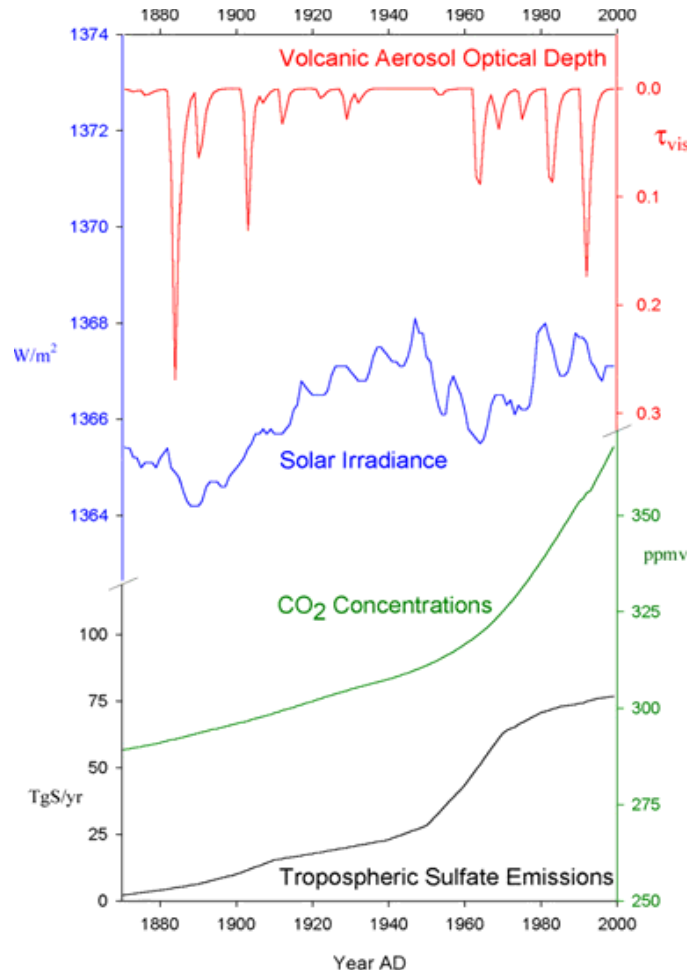


Figure 1: Specified boundary conditions, from top to bottom: Annual average aerosol optical depth at $0.5 \mu\text{m}$ for the stratosphere (red); Hoyt and Schatten (1993) solar irradiance change at top of the atmosphere (blue); CO_2 concentration (green); anthropogenic emission rate of sulfur used for scaling a seasonal distribution from Rasch et al. (2000). Not shown are changes in other greenhouse gases (see text).

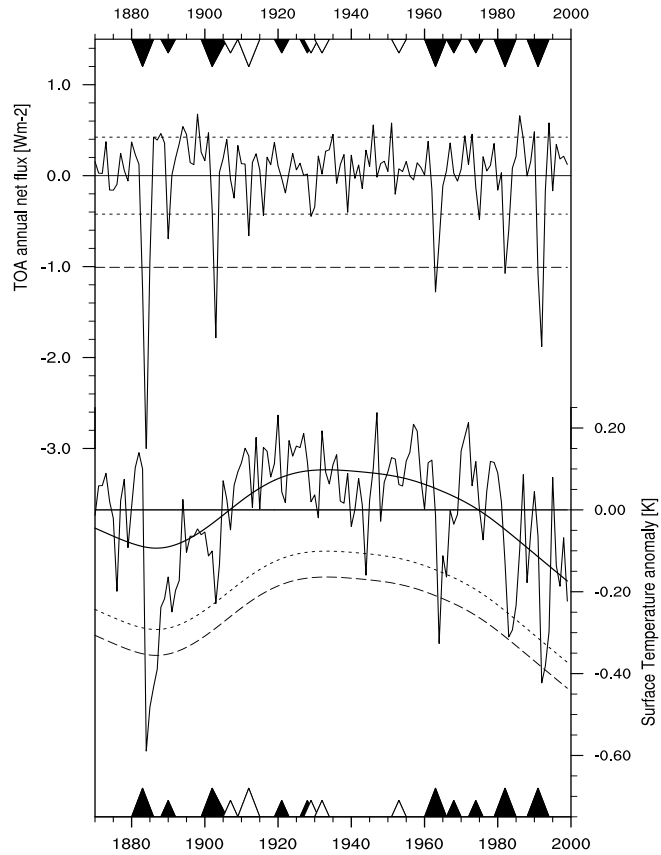


Figure 2: Top: The volcanic forcing is shown as the actual change in TOA radiative balance in VOL in response to aerosol and climatic perturbations. Bottom: Global annual surface temperature evolution with fitted cubic spline and added -2σ intervals from CON (short dashed, no volcanoes included) and VOL (including the volcanoes).

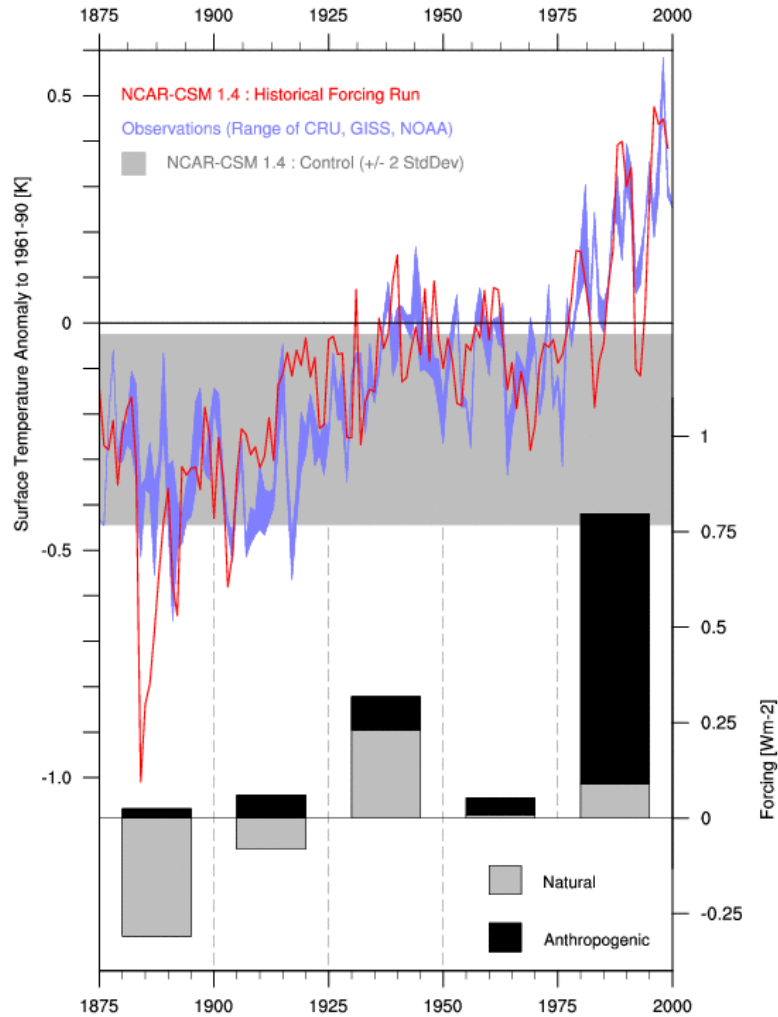


Figure 3: Top: Annual average anomalies (reference 1961-1990) compared to the 2σ range of CON (gray box) and to observational datasets of Jones et al. (2001), Hansen et al. (1999) and Quayle et al. (1999) shown in blue. Bottom: 25-year averaged combined natural (volcanic and solar) and anthropogenic forcing. See text for details.

Sulfate Aerosol Loading vs Temperature Decrease

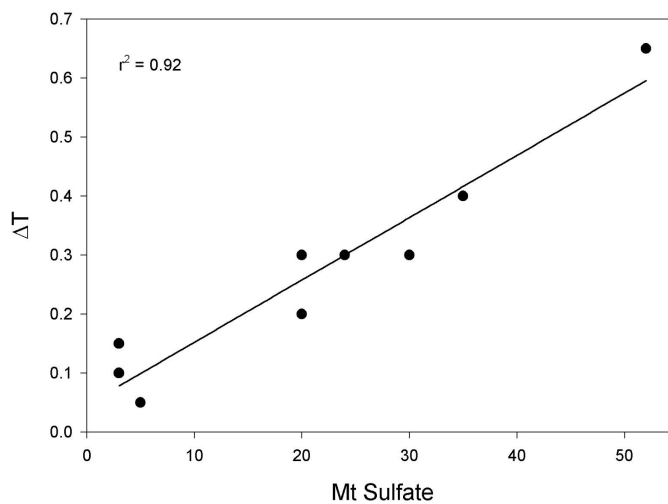


Figure 4: Mass of maximum sulfuric acid in the model versus maximum temperature reduction. Note: The temperature change is an estimate with at least $\pm 0.1^\circ$ uncertainty due to internal variability.

Table Captions

Table 1 **NAO - Observations:** NAO indices calculated after Hurrell (1995) for five years around the seven the largest volcanic eruptions as simulated in VOL and HIST. The evolution of the NAO is compared to the observations of Hurrell (1995) (updated). Added are also the superposed NAO indices from four short ensemble simulations of the large Krakatau eruption (KRA).

Year	VOL	HIST	Hurrell	KRA
-1	-1.05	-0.16	1.38	-
0	0.55	-0.79	-0.06	0.11
1	0.57	0.26	1.43	1.00
2	0.96	0.54	0.01	0.20
3	0.27	0.02	-0.23	-0.75

Table 1: **NAO - Observations:** NAO indices calculated after Hurrell (1995) for five years around the seven the largest volcanic eruptions as simulated in VOL and HIST. The evolution of the NAO is compared to the observations of Hurrell (1995) (updated). Added are also the superposed NAO indices from four short ensemble simulations of the large Krakatau eruption (KRA).